E-ChRPs: Engineered Chromatin Remodeling Proteins for Precise Nucleosome Positioning

Authors/Affiliations

Donovan DA[1&], Crandall JG[1&], Banks OGB[1], Jensvold ZD[1], McKnight LE[1], McKnight JN[1,2*]

1 Institute of Molecular Biology, University of Oregon, Eugene OR 97403
2 Department of Biology, University of Oregon, Eugene OR 97403
[&]These authors contributed equally to this work.
*Correspondence: jmcknig2@uoregon.edu

Abstract

Regulation of chromatin structure is essential for controlling the access of DNA to factors that require association with specific DNA sequences. Here we describe the development of engineered chromatin remodeling proteins (E-ChRPs), which can precisely alter positions of target nucleosomes throughout the genome. E-ChRPs are highly versatile and capable of blocking access of DNA sequences to endogenous DNA binding proteins, thus providing a means to investigate and manipulate DNA-dependent processes.

Main Body

The nucleosome is the fundamental unit of chromatin, composed of DNA wrapped around an octamer of histone proteins. While nucleosomes are dynamic structures that are constantly assembled, disassembled, and moved around the genome, their positions at gene regulatory elements like transcription start sites (TSSs) show characteristic organization[1]. Thus, nucleosome positions are thought to have regulatory implications for DNA-dependent processes like transcription, replication and DNA repair[2-4]. Because positions of nucleosomes in the genome play a major role in determining DNA sequence accessibility, the ability to precisely manipulate nucleosome positions would have profound implications for understanding and controlling DNA-dependent processes in cells. Here we have designed and validated the function of engineered chromatin remodeling proteins (E-ChRPs) to precisely reposition nucleosomes in a sequence-dependent manner in an otherwise native genomic context.

The core E-ChRP design was derived from previous work[5,6] where individual sequence-specific DNA binding domains (DBDs) replaced the C-terminal nonspecific DNA binding domain of a functional *S. cerevisiae* Chd1 chromatin remodeler fragment (Fig. 1a). Yeast Chd1 is an ideal enzyme for engineered chromatin remodeling because it is monomeric, displays robust nucleosome positioning activity on nucleosome substrates derived from various sources, and is less influenced by histone modifications than other chromatin remodeling enzymes[7,8]. We incorporated unique restriction sites flanking the fused DNA binding domain in vectors for recombinant expression in *E. coli*, constitutive expression from ADH1, TEF or GPD promoters in *S. cerevisiae*[9], or galactose-inducible expression from the HO locus in *S. cerevisiae*[10].

We first tested mononucleosome targeting of multiple E-ChRPs with various DNA binding domains. To determine if these E-ChRPs were properly recruited to target nucleosomes *in vitro,* we generated end-

positioned mononucleosomes assembled on the 601-positioning sequence[11] with 125 base pairs of flanking DNA. The extranucleosomal DNA either contained or lacked a consensus binding motif corresponding to multiple E-ChRPs harboring distinct DNA binding domains. E-ChRPs containing DNA binding domains from *E. coli* AraC, *S. pombe* Res1, *D. melanogaster* Engrailed, or *R. norvegicus* Glucocorticoid Receptor (GR) were able to mobilize nucleosomes containing their respective recruitment motifs but were inactive on nucleosomes lacking motifs (Fig. 1b). Fusion of the native, sequence-nonspecific DBD from Chd1 to our E-ChRP scaffold showed no apparent discrimination against DNA sequences, and was capable of fully mobilizing the nonspecific mononucleosome control (Fig. 1b, lanes 28-30).

We next examined whether the addition of a flexible linker between the Chd1 remodeler core and DNA binding domain increased the effective reach of our E-ChRPs. We first tested the ability of an E-ChRP with a DBD from the *S. cerevisiae* meiotic repressor Ume6 to move mononucleosomes containing a recognition motif 20 or 40 base pairs from the nucleosome edge (Supplementary Fig. 1a). Without a flexible linker, the Chd1-Ume6 E-ChRP was active exclusively when the motif was 20bp away. In contrast, addition of eleven repeats of glycine-glycine-serine (GGSx11) allowed the remodeler to efficiently mobilize both nucleosome substrates. Consistent with this increased reach *in vitro*, the Ume6 E-ChRP containing a GGSx11 linker positioned a larger fraction of nucleosomes onto target sequences across the *S. cerevisiae* genome (Fig. 1c, Supplementary Fig. 1b). Because the flexible linker led to more robust E-ChRP activity and our design was compatible with multiple fusions *in vitro* and *in vivo* (Fig. 1b, Supplementary Fig. 2), we selected this general scaffold for all subsequent experiments.

To gain temporal control of E-ChRPs *in vivo*, we introduced the Ume6 E-ChRP under the control of a galactose-inducible promoter in yeast. Prior to addition of galactose, endogenous Ume6 associates with

its consensus sequence (URS1) across the genome and positions motif-proximal nucleosomes leaving 30 bp between the nucleosome edge and URS1 motif [6,12]. After galactose induction of the Ume6 E-ChRP, a majority of nucleosomes nearest the URS1 site are efficiently repositioned to occlude the URS1 motif within the 120 minute induction period. This galactose-inducible approach allows for more complete remodeling of nucleosomes than the same E-ChRP under the control of a constitutively active ADH1 promoter (Fig. 1d).

We reasoned that because the post-induction nucleosome position results in the recruitment motif becoming buried within nucleosomal DNA, remodeling should interfere with binding of endogenous Ume6 (Fig. 1e). To test this possibility, we tagged endogenous Ume6 with a FLAG epitope and measured Ume6-FLAG binding by ChIP-seq before and after induction of the Ume6 E-ChRP. Prior to induction, Ume6-FLAG binding was observed at URS1 sites across the genome (Supplementary Fig. 3a). After induction of the Ume6 E-ChRP, nucleosomes were shifted over URS1 sites and Ume6 binding was reduced at many genomic locations (Supplementary Fig. 3a). When we separated Ume6 binding sites based on whether proximal nucleosome positions were affected by the Ume6 E-ChRP, we noticed that loss of Ume6-FLAG signal was strikingly reduced where nucleosomes were shifted, but minimally reduced where nucleosomes were not shifted (Fig. 1e, Supplementary Fig. 3b). To verify that this reduction in Ume6-FLAG signal was not due to direct binding competition with the E-ChRP DNA binding domain, we measured Ume6-FLAG ChIP signal in the presence of a catalytically inactive Ume6 E-ChRP. This construct, which cannot move nucleosomes but should retain the capacity to interact with Ume6 binding sites, did not similarly reduce Ume6-FLAG signal (Fig. 1e, Supplementary Fig. 3a). Thus, E-ChRPs can inducibly move nucleosomes over target sequences to restrict access of the underlying DNA.

One limitation of the above-described E-ChRPs is their need to compete with endogenous factors for binding sites. To circumvent this problem, we created an E-ChRP composed of the Spycatcher protein fused to the C-terminus of the Chd1 E-ChRP scaffold. Spycatcher specifically recognizes a short (~1kDa) Spytag epitope, forming an isopeptide linkage that allows covalent protein fusions to be created *in vitro* and *in vivo*[13]. This fusion provides two major potential improvements to the E-ChRP system. First, by appending Spytag to a transcription factor of interest, nucleosome positioning can be achieved by a single E-ChRP without the need to design new DBD fusions (Fig. 2a). Second, by tagging a transcription factor at its endogenous locus, the protein becomes a targetable element for the Spycatcher E-ChRP (Fig. 2a). This bypasses the requirement of a vacant DNA binding site to target a DBD-containing E-ChRP, allowing access to sequences in the genome that were blocked by a bound transcription factor. In sum, this strategy produces a single Spycatcher E-ChRP that can be targeted to any chromatin-bound protein of interest in the genome by simple attachment of a short Spytag (Fig. 2a).

To validate the function of the Spycatcher E-ChRP design, we purified recombinantly-expressed Chd1-Spycatcher and two Spytag-containing DNA binding domains. Mononucleosomes harboring recognition sequences for each DNA binding domain in the extranucleosomal DNA were incubated with the Spycatcher E-ChRP with and without addition of Spytag-Engrailed(DBD) or Spytag-AraC(DBD). The Spycatcher E-ChRP has no activity on nucleosome substrates in the absence of a Spytag-DBD pair (Fig. 2b, lanes 2-4), since Spycatcher has no intrinsic DNA binding affinity. However, addition of either Spytag-AraC(DBD) (Fig. 2b, lanes 5-7) or Spytag-Engrailed(DBD) (Fig. 2b, lanes 8-10) resulted in robust repositioning of mononucleosomes *in vitro*, demonstrating the versatility of this system. We next introduced the Spycatcher E-ChRP under a constitutive ADH1 promoter into *S. cerevisiae* cells where a C-terminal Spytag was added to full-length Ume6 at the endogenous locus. As expected, we observed

repositioned nucleosomes at URS1 sites across the genome indicating that chromatin remodeling was localized to Ume6-bound loci (Fig. 2c).

To achieve temporal control of this versatile system *in vivo*, we appended Spytag to the C-terminus of either Ume6 or Reb1, a yeast general regulatory factor, in a strain harboring a galactose-inducible Spycatcher E-ChRP at the HO locus. After induction of Spycatcher E-ChRP expression, nucleosomes were shifted toward Ume6 binding sites in cells containing Ume6-Spytag or toward Reb1 binding sites in cells containing Reb1-Spytag (Fig. 2d, Supplementary Fig. 4a,b). Interestingly, the fraction of shifted nucleosomes was generally low at Ume6 binding sites in Ume6-Spytag cells but comparatively higher at Reb1 binding sites in Reb1-Spytag strains (Fig. 2d). This difference could be explained by higher occupancy or stability of Reb1 binding than Ume6 binding at target sites, which would allow a greater fraction of Reb1-tethered Spycatcher to mobilize motif-proximal nucleosomes. Consistent with this possibility, the abundance of Ume6 is significantly lower than that of Reb1[14]. For both Reb1-Spytag and Ume6-Spytag, the positioning of a single motif-proximal nucleosome by the Spycatcher E-ChRP was capable of initiating the shift of an entire array of nucleosomes toward the target motif (Supplementary Fig. 4b,c).

Interestingly, the positioning of nucleosomes appeared to occur on only the 5' side of the Reb1 recognition sequence, suggesting the directional orientation of Reb1 binding impacts the ability of Chd1 to reach nucleosomes near binding sites (Fig. 2d, Supplementary Fig. 4c). This restriction could be explained by a constrained C-terminus of Reb1 when bound to chromatin, which is consistent with constrained Reb1-MNase cleavage in previous ChEC-seq experiments[15]. Unexpectedly, the fraction of nucleosomes shifted at Reb1 binding sites varied greatly in our data set, with some sites exhibiting repositioning of nearly 100% of motif-proximal nucleosomes in the population and others having a much

smaller fraction moved (Supplementary Fig. 5a). These differences are not explained by initial nucleosome occupancy or location differences (Supplementary Fig. 5b,c), but are possibly related to relative Reb1 occupancy at different genomic locations. Minimally, the observation that all nucleosomes are shifted at some Reb1 binding sites in a population of cells argues that some Reb1 sites are nearly 100% occupied, as E-ChRP-derived nucleosome movement can not be observed without Reb1 binding (Supplementary Fig. 5c). While these Reb1 occupancy estimates are conflated with presence, accessibility and relative occupancy of motif-proximal nucleosomes, our data suggest that Spycatcher E-ChRP can serve as a measure of protein localization in cells that is completely orthogonal to ChIP allowing for a lower-limit estimate of Spytagged protein occupancy at individual binding motifs in the genome.

In conclusion, we have created and validated the use of E-ChRPs as an easy and versatile method for altering the positions of desired nucleosomes both *in vitro* and *in vivo*. We have demonstrated widespread compatibility of various targeting schemes with this approach and have created a single Spycatcher E-ChRP that can be inducibly coupled to chromatin associated factors to move nearby nucleosomes to defined final locations. Furthermore, we have shown the ability of E-ChRPs to precisely establish new nucleosomal arrays and inducibly occlude transcription factor binding motifs across the genome. We envision future research can utilize E-ChRPs to probe significant questions relating the position of nucleosomes on downstream biological processes and can lead to insight into how cells can tolerate or correct ectopic nucleosome positioning events. Finally, the ability to position nucleosomes onto target sequences could potentially lead to the development of E-ChRPs that block oncogenic or other disease-related transcription factors from accessing binding sites genome-wide.

Methods

Plasmids, Strains, and Growth Conditions

The initial Ume6 E-ChRP scaffold was prepared by Gibson assembly[16] in p416-ADH1[9] to include an N-terminal NLS (KKKRK), residues 118-1000 of *S. cerevisiae* Chd1, nine repeats of glycine-glycine-serine, residues 1001-1014 of *S. cerevisiae* Chd1, two additional repeats of glycine-glycine-serine, an AfeI restriction site, residues 764-836 from S. cerevisiae Ume6 and a HindIII restriction site. An analogous backbone was also created with residues 118-1000 of *S. cerevisiae* Chd1 linked directly to the two glycine-glycine-serine repeats followed by AfeI, Ume6 DBD, and HindIII site. Cloning vectors were created in pDEST17, p416-TEF, p416-GPD, p426-ADH1, p426-TEF, p426-GPD and HO-pGAL-poly-KanMX4-HO[10] (a gift from David Stillman, Addgene 51664) to swap the C-terminal Ume6 domain with other targeting domains using AfeI/HindIII restriction cloning or sticky-end PCR[17]. Fusions used in this study include *S. cerevisiae* Ume6 (764-836, cloned from yeast genomic DNA), *D. melanogaster* Engrailed (454-543, cloned from fly genomic DNA), *S. pombe* Res1 (1-147, cloned from a gBlock), *R. norvegicus* Glucocorticoid Receptor (428-513, cloned from a gBlock), *E. coli* AraC (175-281) and the Spycatcher domain[13] (a gift from Mark Howarth, Addgene 35044). Non-integrating plasmids (p416- or p426-) were transformed into *S. cerevisiae* strain W303 (RAD5+) and grown in SD -Ura overnight, diluted to OD_{600}=0.2 in YPD and grown to OD_{600}=0.6-0.8 for chromatin analysis. For galactose induction of E-ChRPs, cells were grown in YP media with 2% raffinose as the sole carbon source. In mid-log phase, raffinose (- induction) or galactose (+ induction) was added to a final concentration of 2% and cells were grown for 2 additional hours at 30°C with shaking. Cells were then fixed and harvested for chromatin analysis. To make Spytagged yeast strains, a C-terminal 3x-FLAG tag followed by the Spytag sequence (AHIVMVDAYKPTK) was added by integration at the endogenous locus for the protein of interest using a selectable drug marker. To recombinantly express Spytagged DNA binding domains for biochemical analysis, domains of

interest were amplified by PCR from source (yeast or fly genomic DNA) followed by restriction cloning into a pDEST-MCS-Spytag vector.

Protein Purification

Chd1 constructs were expressed from pDEST17 vectors (Invitrogen) as previously described[8]. Briefly, proteins were expressed in BL21(DE3) cells, with the RIL plasmid (Stratagene) to aid expression and a plasmid expressing the Trigger Factor chaperone (a kind gift from Li Ma and Guy Montelione) to improve solubility. After induction with 300uM isopropyl-D-thiogalactopyranoside (IPTG) and growth at 18°C for 16 h, cells were lysed by sonication in 500 mM NaCl, 10% glycerol, and 25 mM Tris, pH 7.8. Lysate was clarified by centrifugation at 25,000xg and soluble protein was purified using Co^{2+} affinity chromatography (TALON column, GE Healthcare) followed by anion-exchange chromatography (Q-FF, GE Healthcare).

Nucleosome Sliding Assay

Recombinant yeast histones were purified as previously described[18] and dialyzed by gradient salt dialysis onto the Widom 601 positioning sequence[11]. Nucleosome sliding was performed at 25°C in sliding buffer (50 mM KCl, 15 mM HEPES, pH 7.8, 10 mM $MgCl_2$, 0.1 mM EDTA, 5% sucrose, 0.2 mg/ml bovine serum albumin [BSA], with or without 5 mM ATP) by incubating 0, 10, 20, 40, or 60nM purified E-ChRP with 30nM reconstituted mononucleosomes for 100 minutes. Spycatcher reactions included 25, 50, or 100nM Chd1-Spycatcher and 0, 50 or 100nM of the Spytagged DNA binding domain with 30nM of labeled mononucleosomes. Unless specifically indicated, mononucleosomes contained E-ChRP recognition sequences in the extranucleosomal DNA. Reactions were quenched by diluting 1:2 with solution containing 3 uM competitor DNA containing E-ChRP recognition sequences and 5% sucrose.

Native PAGE (6%) was used to separate the positioning of the mononucleosomes, with Cy5.5-labeled nucleosomal DNA detected by a LiCor Odyssey FC imager.

Micrococcal Nuclease Digestions and Library Construction

Micrococcal nuclease digestions were performed as previously described[19]. Briefly, cells were grown to mid-log phase and fixed with 1% formaldehyde. Chromatin was digested with 10, 20, and 40 units of MNase for 10 minutes. Proper nuclease digestion of DNA was analyzed by agarose gel and samples with approximately 80% mononucleosomes were selected for library construction. After crosslink reversal, RNase treatment, Calf Intestine Phosphatase (CIP, NEB) treatment and Proteinase K digestion, mononucleosome-sized fragments were gel-purified and used to construct libraries with the NuGEN Ovation Ultralow kit per the manufacturer's instructions. Libraries were sequenced at the University of Oregon's Genomics and Cell Characterization Core Facility on an Illumina NextSeq 500 on the 37 cycle, paired-end, High Output setting, yielding approximately 20 million paired reads per sample.

Chromatin Immunoprecipitation and Library Construction

Chromatin immunoprecipitation was performed as previously described[19]. Briefly, cells were grown to mid-log phase, fixed with 1% formaldehyde, and lysed by bead-beating in the presence of protease inhibitors. Chromatin was fragmented by shearing in a Bioruptor sonicator (Diagenode) for a total of 30 minutes (high output, 3x10' cycles of 30 sec. on, 30 sec. off). Sonication conditions were optimized to produce an average fragment size of ~300 basepairs. FLAG-tagged protein was immunoprecipitated using FLAG antibody (Sigma) and Protein G magnetic beads (Invitrogen). After crosslink reversal and Proteinase K digestion, DNA was purified using Qiagen MinElute columns and quantified by Qubit High-Sensitivity fluorometric assay. Libraries were prepared using the NuGEN Ovation Ultralow kit by the manufacturer's instructions and sequenced at the University of Oregon's Genomics and Cell

Characterization Core Facility on an Illumina HiSeq4000 with 50 or 100 cycles of single-end setting, yielding approximately 15 million reads per sample.

Data Processing and Analysis

MNase sequencing data were analyzed as described previously[6,20,21]. Briefly, paired-end reads were aligned to the *S. cerevisiae* reference genome[22] with Bowtie 2[23], and filtered computationally for unique fragments between 100 and 200 bp. Dyad positions were calculated as the midpoint of paired reads, then dyad coverage was normalized across the *S. cerevisiae* genome for an average read/bp of 1.0. Nucleosome alignments to transcription factor binding sites were performed by taking average dyad signal at each position relative to all intergenic instances of a motif center. Motifs were obtained from the JASPAR database[24] and intergenic instances were found using the Saccharomyces Genome Database Pattern Matching tool (http://www.yeastgenome.org/cgi-bin/PATMATCH/nph-patmatch). For ChIP-seq data, single-end reads were aligned to the *S. cerevisiae* reference genome with Bowtie 2 and total read coverage was normalized such that the average read at a genomic location was 1.0. ChIP peaks were called using a 400 bp sliding window with a threshold average enrichment within the window of 4.0.

Figure Legends

Figure 1. Development and Validation of E-ChRPs with Fused DNA Binding Domains. (a) Schematic representation of E-ChRP design with Chd1 remodeling core, flexible GGS linker, and targeting domains derived from various organisms used in this study. (b) Nucleosome sliding assay demonstrating functionality of increasing concentrations of E-ChRPs containing AraC DBD (lanes 1-5, 22-24), Res1 DBD (lanes 6-10, 25-27), Engrailed DBD (lanes 11-15), Glucocorticoid Receptor DBD (lanes 16-20) or Chd1 endogenous DBD (lanes 28-30) *in vitro*. Nucleosomes in lanes 1-20 possess recognition motifs in

extranucleosomal DNA for the respective E-ChRP while lanes 21-30 have no recognition motif. Lower electrophoretic mobility indicates repositioning of nucleosomes away from their end positions. (c) Average nucleosome dyad position at intergenic Ume6 binding motifs (URS1) in *ume6* cells in the presence or absence of Ume6 E-ChRPs with or without a flexible GGSx11 linker. (d) Representative Ume6 E-ChRP target demonstrating positioning of nucleosomes toward motif by galactose-inducible Ume6 E-ChRP or a constitutively expressed E-ChRP under the ADH1 promoter. (e) Cartoon depiction of Ume6 E-ChRP activity blocking association of endogenous Ume6 at target sites (left) and representative examples E-ChRP targets where endogenous Ume6 is removed (top) or not removed (bottom) after galactose induction of Ume6 E-ChRP. The catalytic null E-ChRP retains a Ume6 DBD but has a Walker B (D513N) substitution in the Chd1 catalytic core.

Figure 2. Development and Validation of E-ChRPs Containing Spycatcher/Spytag Pairs. (a) Cartoon representation for introducing a Chd1-Spycatcher E-ChRP into cells containing Spytagged chromatin-bound proteins. The Spycatcher domain forms a covalent isopeptide bond with Spytag allowing for localization of E-ChRP activity to endogenously-bound transcription factors. (b) Nucleosome sliding assay demonstrating that a single Spycatcher E-ChRP cannot position nucleosomes without a Spytag-containing DBD (lanes 2-4) but can use a Spytagged AraC DBD (lanes 5-7) or Engrailed DBD (lanes 8-10) to reposition nucleosomes containing respective DBD recognition motifs. (c) Representative motif where ADH1-driven Spycatcher E-ChRP can reposition nucleosomes at a Ume6 binding site in the presence of Ume6-Spytag (left) and genomic analysis of nucleosome positioning by Spycatcher E-ChRP at 202 intergenic instances of the Ume6 recognition sequence in cells containing Spytagged Ume6 (right). (d) Genomic analysis of nucleosome positions in Reb1-Spytagged cells (left) or Ume6-Spytagged cells (right) before and after 2-hour induction of galactose-inducible Spycatcher E-ChRP. Heat maps show change in

nucleosome dyad signal after induction of Spycatcher E-ChRP while individual traces show positions of nucleosomes before and after Spycatcher E-ChRP induction for each Spytag-DBD strain.

Author Contributions

L.E.M., Z.D.J., and J.N.M. conceived, designed and cloned the E-ChRP core. L.E.M., Z.D.J., D.A.D., J.G.C., and O.G.B.B. cloned subsequent E-ChRPs. D.A.D. performed all protein purifications and nucleosome sliding assays for DBD E-ChRPs and Spycatcher E-ChRPs. J.G.C. performed induction experiments and prepared MNase-seq and ChIP-seq libraries for DBD E-ChRPs. O.G.B.B. performed induction experiments and prepared MNase-seq libraries for Spycatcher E-ChRPs. Z.D.J. and L.E.M. purified all core histones. D.A.D. and J.N.M. reconstituted histone octamers and mononucleosomes. J.N.M. performed bioinformatics and data analysis. D.A.D., J.G.C., O.G.B.B. and J.N.M. wrote the manuscript. J.N.M. and L.E.M. supervised the work. All authors read and approved the final manuscript. D.A.D. and J.G.C. contributed equally to this work.

Acknowledgements

We would like to thank the Bowman Lab (Johns Hopkins University) for histone plasmids and Chd1 constructs, the Tsukiyama lab (Fred Hutchinson Cancer Research Center) and Zentner lab (Indiana University) for selectable epitope tagging vectors and the Doe Lab (University of Oregon) for a fly genomic DNA extraction protocol. This work was supported by a National Institutes of Health training grant T32 GM007759 (to D.A.D. and O.G.B.B.), by a National Institutes of Health training grant T32 GM007413 (to D.A.D.) and by the Donald and Delia Baxter Foundation (J.N.M.).

References

1 Lai, W. K. M. & Pugh, B. F. Understanding nucleosome dynamics and their links to gene expression and DNA replication. *Nat Rev Mol Cell Biol* **18**, 548-562, doi:10.1038/nrm.2017.47 (2017).

2 Hauer, M. H. & Gasser, S. M. Chromatin and nucleosome dynamics in DNA damage and repair. *Genes Dev* **31**, 2204-2221, doi:10.1101/gad.307702.117 (2017).

3 MacAlpine, D. M. & Almouzni, G. Chromatin and DNA replication. *Cold Spring Harb Perspect Biol* **5**, a010207, doi:10.1101/cshperspect.a010207 (2013).

4 Venkatesh, S. & Workman, J. L. Histone exchange, chromatin structure and the regulation of transcription. *Nat Rev Mol Cell Biol* **16**, 178-189, doi:10.1038/nrm3941 (2015).

5 McKnight, J. N., Jenkins, K. R., Nodelman, I. M., Escobar, T. & Bowman, G. D. Extranucleosomal DNA binding directs nucleosome sliding by Chd1. *Mol Cell Biol* **31**, 4746-4759, doi:10.1128/MCB.05735-11 (2011).

6 McKnight, J. N., Tsukiyama, T. & Bowman, G. D. Sequence-targeted nucleosome sliding in vivo by a hybrid Chd1 chromatin remodeler. *Genome Res* **26**, 693-704, doi:10.1101/gr.199919.115 (2016).

7 Ferreira, H., Flaus, A. & Owen-Hughes, T. Histone modifications influence the action of Snf2 family remodelling enzymes by different mechanisms. *J Mol Biol* **374**, 563-579, doi:10.1016/j.jmb.2007.09.059 (2007).

8 Hauk, G., McKnight, J. N., Nodelman, I. M. & Bowman, G. D. The chromodomains of the Chd1 chromatin remodeler regulate DNA access to the ATPase motor. *Mol Cell* **39**, 711-723, doi:10.1016/j.molcel.2010.08.012 (2010).

9 Mumberg, D., Muller, R. & Funk, M. Yeast vectors for the controlled expression of heterologous proteins in different genetic backgrounds. *Gene* **156**, 119-122 (1995).

10 Voth, W. P., Richards, J. D., Shaw, J. M. & Stillman, D. J. Yeast vectors for integration at the HO locus. *Nucleic Acids Res* **29**, E59-59 (2001).

11 Lowary, P. T. & Widom, J. New DNA sequence rules for high affinity binding to histone octamer and sequence-directed nucleosome positioning. *J Mol Biol* **276**, 19-42, doi:10.1006/jmbi.1997.1494 (1998).

12 Goldmark, J. P., Fazzio, T. G., Estep, P. W., Church, G. M. & Tsukiyama, T. The Isw2 chromatin remodeling complex represses early meiotic genes upon recruitment by Ume6p. *Cell* **103**, 423-433 (2000).

13 Zakeri, B. *et al.* Peptide tag forming a rapid covalent bond to a protein, through engineering a bacterial adhesin. *Proc Natl Acad Sci U S A* **109**, E690-697, doi:10.1073/pnas.1115485109 (2012).

14 Kulak, N. A., Pichler, G., Paron, I., Nagaraj, N. & Mann, M. Minimal, encapsulated proteomic-sample processing applied to copy-number estimation in eukaryotic cells. *Nat Methods* **11**, 319-324, doi:10.1038/nmeth.2834 (2014).

15 Zentner, G. E., Kasinathan, S., Xin, B., Rohs, R. & Henikoff, S. ChEC-seq kinetics discriminates transcription factor binding sites by DNA sequence and shape in vivo. *Nat Commun* **6**, 8733, doi:10.1038/ncomms9733 (2015).

16 Gibson, D. G. *et al.* Enzymatic assembly of DNA molecules up to several hundred kilobases. *Nat Methods* **6**, 343-345, doi:10.1038/nmeth.1318 (2009).

17 Walker, A., Taylor, J., Rowe, D. & Summers, D. A method for generating sticky-end PCR products which facilitates unidirectional cloning and the one-step assembly of complex DNA constructs. *Plasmid* **59**, 155-162, doi:10.1016/j.plasmid.2008.02.002 (2008).

18 Luger, K., Rechsteiner, T. J. & Richmond, T. J. Expression and purification of recombinant histones and nucleosome reconstitution. *Methods Mol Biol* **119**, 1-16, doi:10.1385/1-59259-681-9:1 (1999).
19 Rodriguez, J., McKnight, J. N. & Tsukiyama, T. Genome-Wide Analysis of Nucleosome Positions, Occupancy, and Accessibility in Yeast: Nucleosome Mapping, High-Resolution Histone ChIP, and NCAM. *Curr Protoc Mol Biol* **108**, 21 28 21-16, doi:10.1002/0471142727.mb2128s108 (2014).
20 McKnight, J. N., Boerma, J. W., Breeden, L. L. & Tsukiyama, T. Global Promoter Targeting of a Conserved Lysine Deacetylase for Transcriptional Shutoff during Quiescence Entry. *Mol Cell* **59**, 732-743, doi:10.1016/j.molcel.2015.07.014 (2015).
21 McKnight, J. N. & Tsukiyama, T. The conserved HDAC Rpd3 drives transcriptional quiescence in S. cerevisiae. *Genom Data* **6**, 245-248, doi:10.1016/j.gdata.2015.10.008 (2015).
22 Cunningham, F. *et al.* Ensembl 2015. *Nucleic Acids Res* **43**, D662-669, doi:10.1093/nar/gku1010 (2015).
23 Langmead, B. & Salzberg, S. L. Fast gapped-read alignment with Bowtie 2. *Nat Methods* **9**, 357-359, doi:10.1038/nmeth.1923 (2012).
24 Khan, A. *et al.* JASPAR 2018: update of the open-access database of transcription factor binding profiles and its web framework. *Nucleic Acids Res* **46**, D1284, doi:10.1093/nar/gkx1188 (2018).

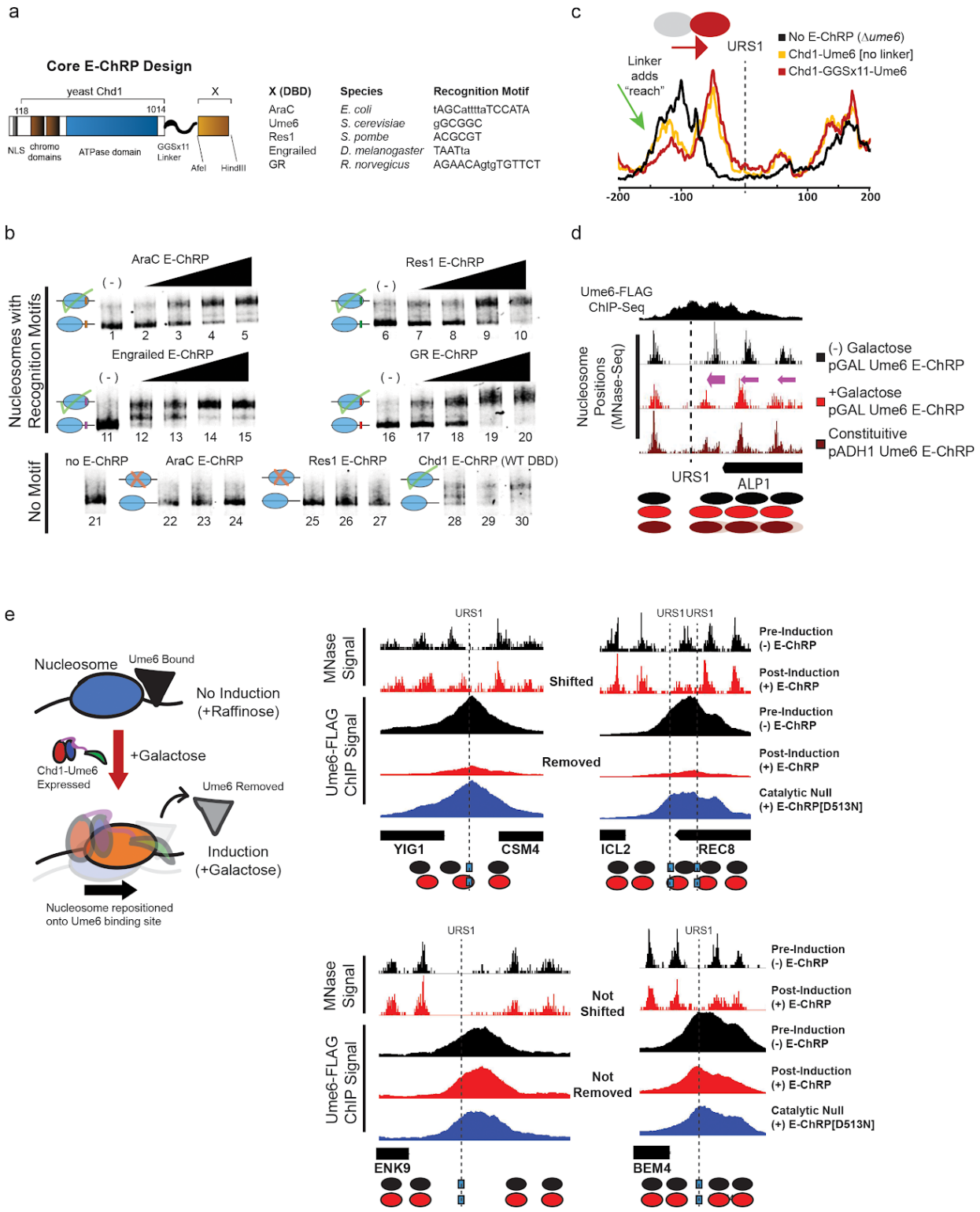

Figure 1. Development and Validation of E-ChRPs with Fused DNA Binding Domains.

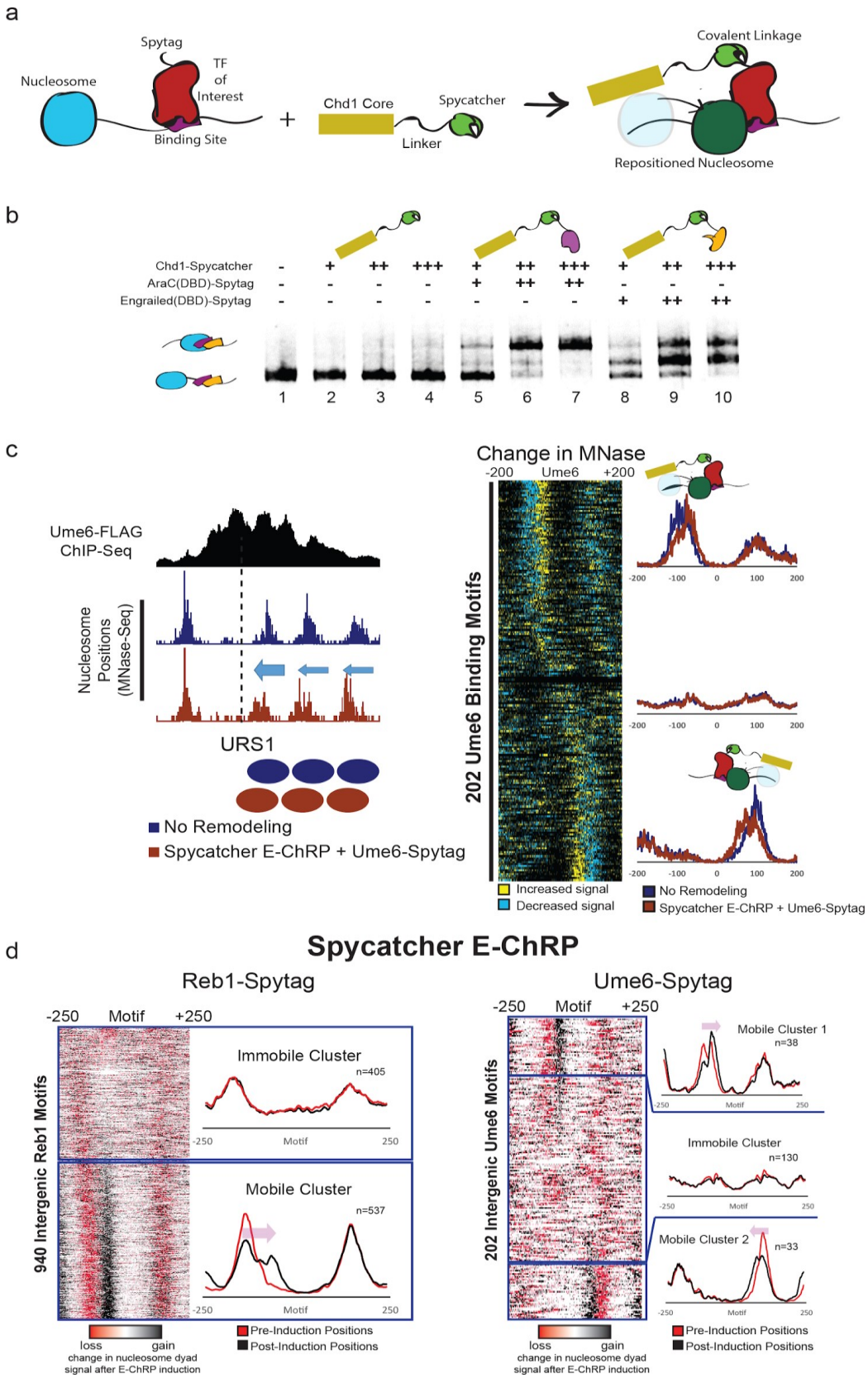

Figure 2. Development and Validation of E-ChRPs Containing Spycatcher/Spytag Pairs.

Supplementary Figures

Supplementary Figure 1. Effect of Flexible GGSx11 Linker on E-ChRP Activity. (a) Nucleosome sliding assay for showing the ability of E-ChRPs with and without a flexible linker to position nucleosomes containing recognition motifs 20 or 40 base pairs from the nucleosome edge (top). Lower electrophoretic mobility indicates movement of the nucleosome toward the positioning sequence. Summary of the ability of each E-ChRP to position nucleosome substrates is provided (bottom). (b) Representative genomic locus showing nucleosome dyad positions in the absence of E-ChRP or presence of E-ChRPs with and without a flexible GGSx11 protein linker. These experiments were performed in a *Δume6* background.

Supplementary Figure 2. Validation of Multiple E-ChRPs in Yeast Cells. Nucleosome dyad positions are shown at representative Ume6 targets (URS1, top) or Engrailed targets (TAAT, bottom) in the presence or absence of Ume6 E-ChRP or Engrailed E-ChRP. Motif-proximal nucleosomes are highlighted next to indicated motifs with blue arrows showing direction of nucleosome movement at target sites. Cartoon representations of nucleosome positions are given for each locus.

Supplementary Figure 3. Inducible Ume6 E-ChRP Globally Prevents Binding of Endogenous Ume6. (a) Genome browser image showing biological replicates of Ume6-FLAG ChIP signal across ChrXVI before (black) and after (red) 2-hour induction Ume6 E-ChRP with galactose. Blue peaks correspond to a Ume6-FLAG ChIP signal in the presence of a catalytically inactive Ume6 E-ChRP containing a Walker B (D513N) substitution in the Chd1 remodeling core. Blue and red highlights correspond to loci depicted in Fig. 1e. (b) Global analysis centered on 600 Ume6-FLAG ChIP peaks for change in nucleosome dyad signal (yellow/blue) after Ume6 E-ChRP induction and associated change in endogenous Ume6-FLAG ChIP signal (blue/red). Clusters represent Ume6 peaks with the highest and lowest change in nucleosome

positioning based on change in MNase signal. Individual average nucleosome dyad signal for each cluster before and after E-ChRP induction is given in blue and orange, respectively. Change in Ume6-FLAG ChIP signal for each cluster is provided in black and gray traces, respectively. Cartoon depiction for each cluster is provided on the right.

Supplementary Figure 4. Inducible Spycatcher E-ChRP Positions Nucleosomes as Directed by Spytagged Factors. (a) Genome browser image showing nucleosome positions before and after induction of Spycatcher E-ChRP in cells containing Ume6-Spytag (top) or Reb1-Spytag (bottom). Location of a proximal Reb1 binding motif or Ume6 binding motif is denoted by a dashed line while directional nucleosome positioning is indicated by blue and red arrows. At this locus, Reb1-Spytag and Ume6-Spytag cause different nucleosomes to be selectively moved by Spycatcher E-ChRP as directed by the location of bound Ume6 or Reb1. (b) Same as (a) showing a locus where Reb1 and Ume6 motifs are located adjacent to each other. In this case, both Reb1-Spytag and Ume6-Spytag allow the Spycatcher E-ChRP to select the same nucleosome but the nucleosome is moved to different final locations based on the predicted location of the individual bound factors. Reb1-Spytag leads to further positioning than Ume6-Spytag because the Reb1 motif is distal to the Ume6 motif. (c) Heat map (left) showing the difference in nucleosome dyad signal +/- 1000 bp from 940 Reb1 motifs after Spycatcher E-ChRP induction in Reb1-Spytag cells. Average change in nucleosome signal after Spycatcher E-ChRP induction at Reb1 motifs where nucleosomes are moved (mobile cluster) or not moved (immobile cluster) are provided (right).

Supplementary Figure 5. Spycatcher E-ChRP Activity Varies at Reb1 Binding Sites. (a) Nucleosome dyad signal at 943 intergenic REB1 motifs from MNase-seq experiments in Reb1-Spytag strains before (left) and after (right) 2-hour induction of Spycatcher E-ChRP with galactose. Rows are ordered by change in

nucleosome positioning after Spycatcher E-ChRP induction. Purple shading highlights the region to where nucleosomes are moved by Spycatcher E-ChRP interacting with Reb1-Spytag. (b) The purple mobile fraction from (a) was split into deciles (~50 motifs per decile) showing average positioning by Spycatcher E-ChRP for each decile. Dashed lines indicate the pre-induction, unremodeled position (red) or post-induction, remodeled position (black). Ume6-Spytag control traces are provided for the top and bottom deciles demonstrating that Spycatcher E-ChRP cannot function at Reb1 sites in the presence of Ume6-Spytag instead of Reb1-Spytag. (c) Genome browser images for representative loci showing positioning by Spycatcher E-ChRP with Reb1-Spytag for the top, middle and bottom deciles. Purple shading indicates the motif-proximal repositioned nucleosomes. Dashed lines indicate the location of Reb1 motif.

Donovan et al Supplementary Figure 1

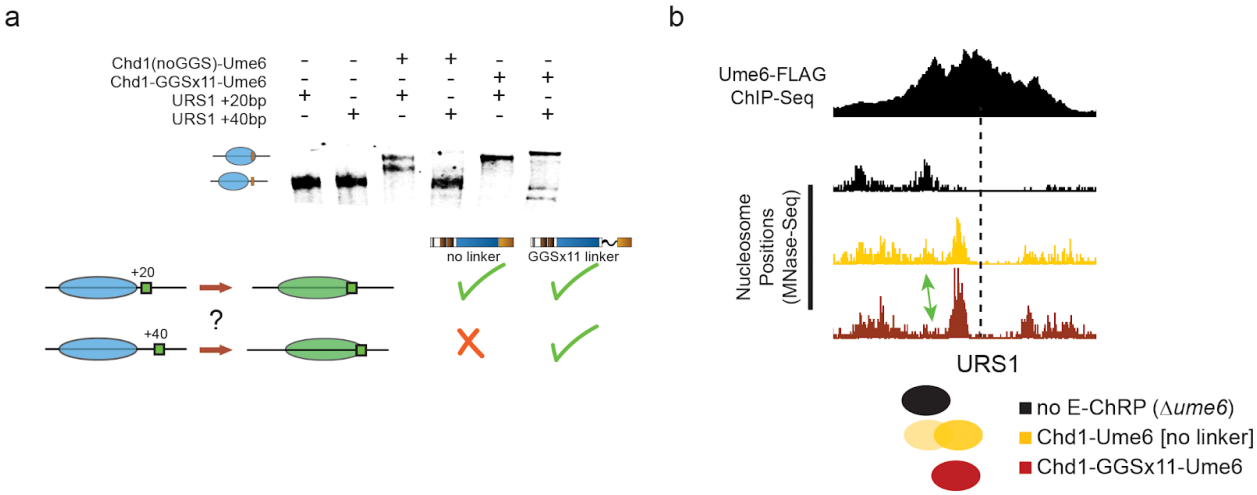

Supplementary Figure 1. Effect of Flexible GGSx11 Linker on E-ChRP Activity.

Donovan et al Supplementary Figure 2

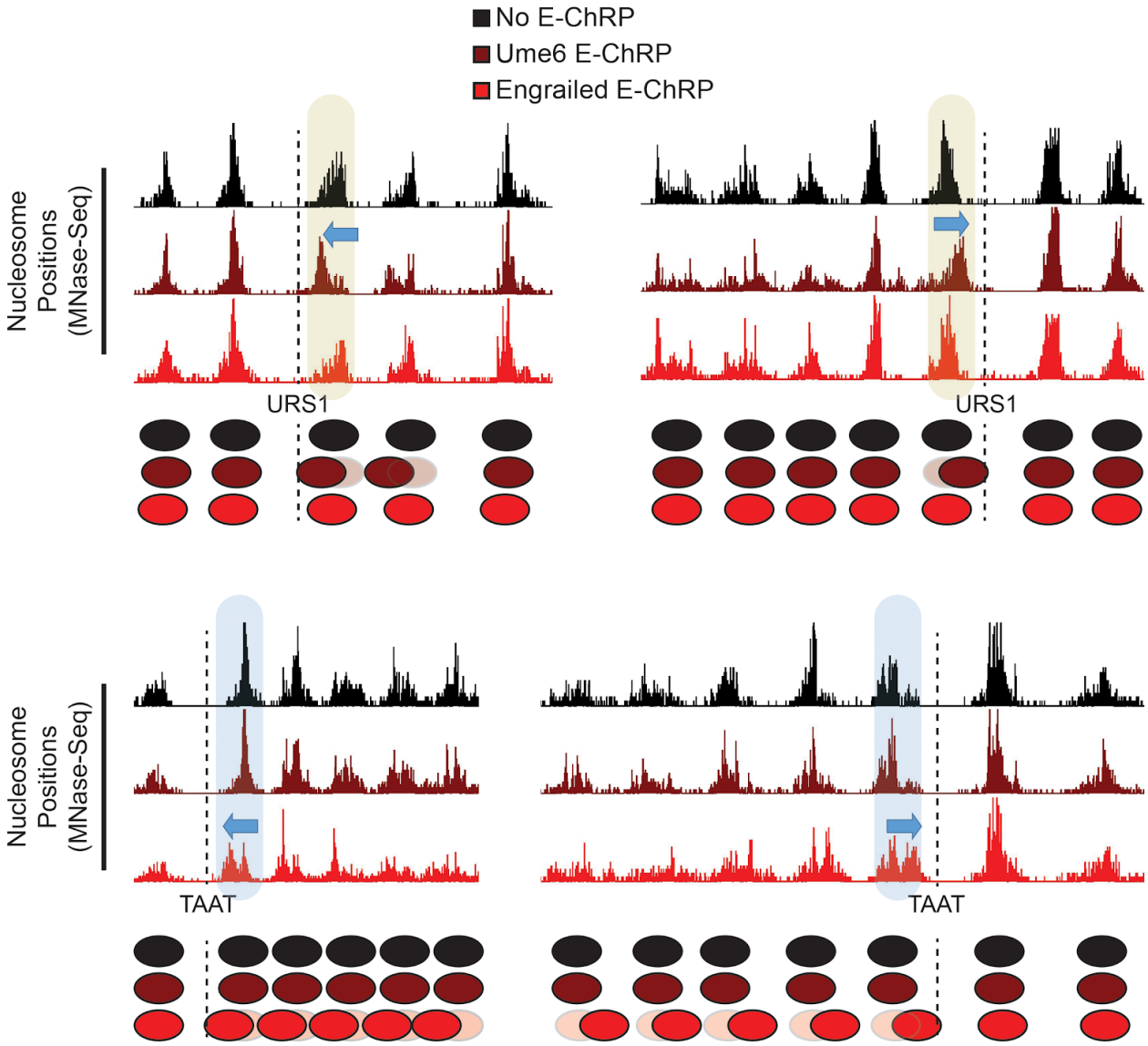

Supplementary Figure 2. Validation of Multiple E-ChRPs in Yeast Cells.

Donovan et al Supplementary Figure 3

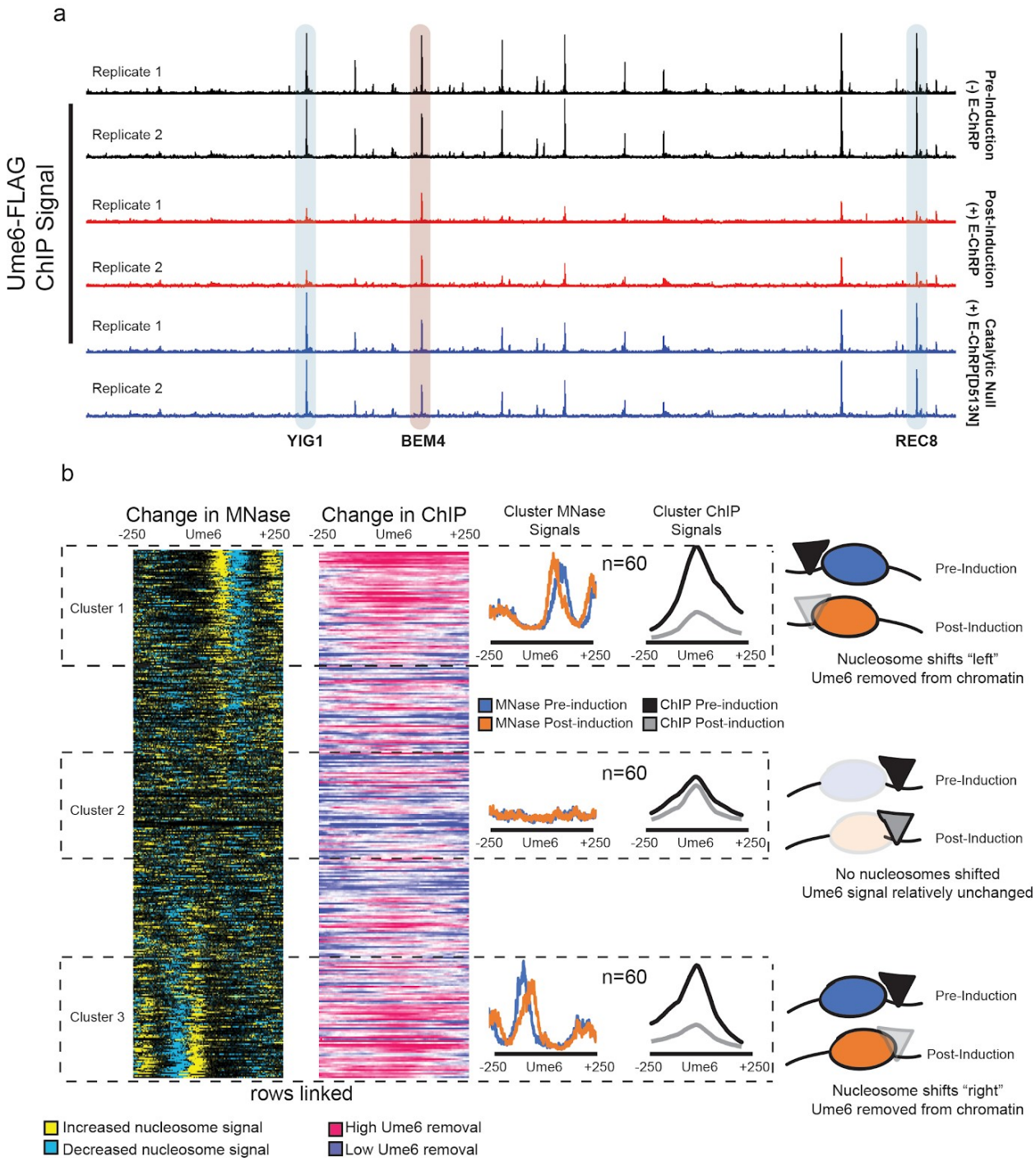

Supplementary Figure 3. Inducible Ume6 E-ChRP Globally Prevents Binding of Endogenous Ume6.

Donovan et al Supplementary Figure 4

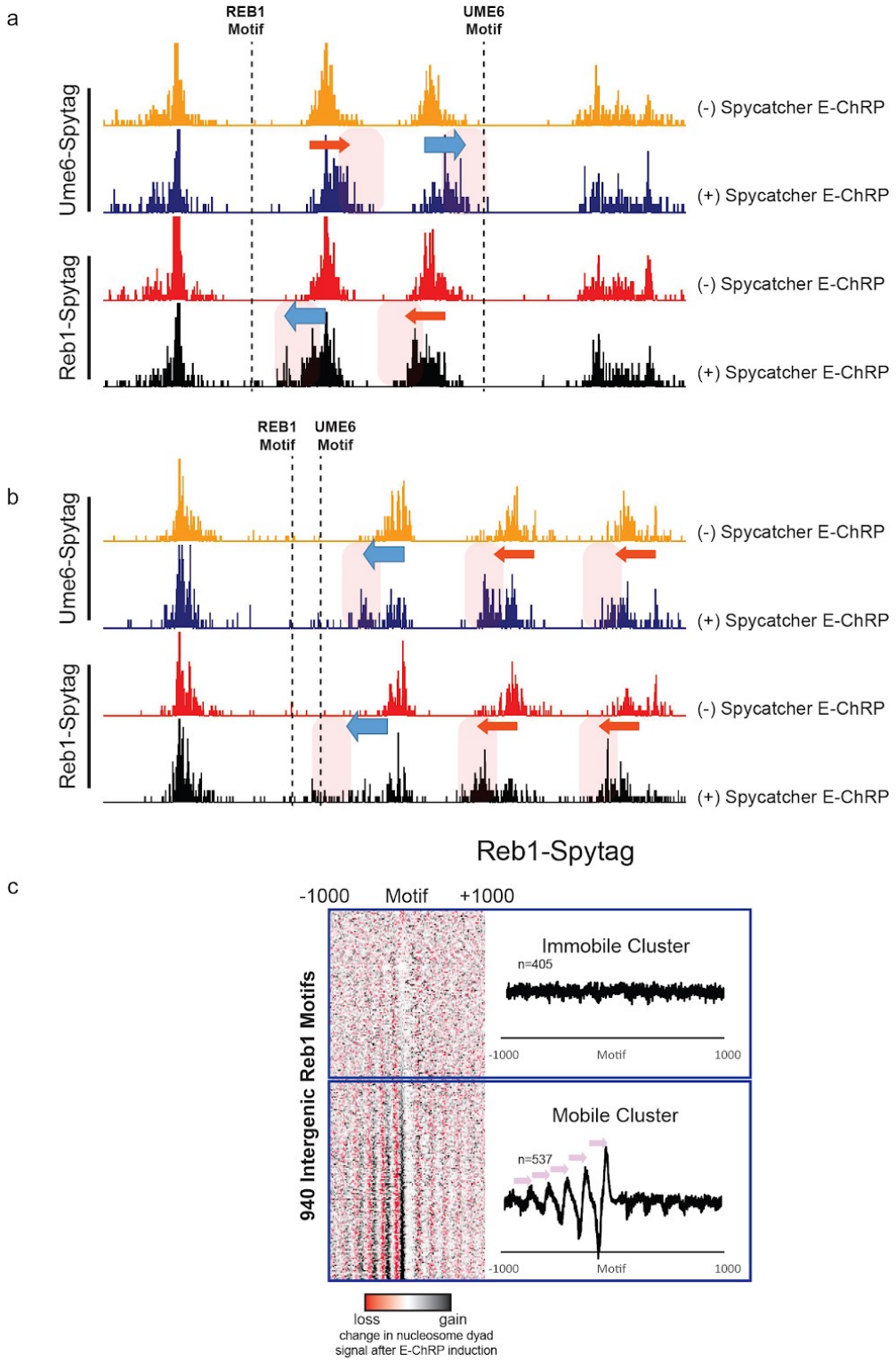

Supplementary Figure 4. Inducible Spycatcher E-ChRP Positions Nucleosomes as Directed by Spytagged Factors.

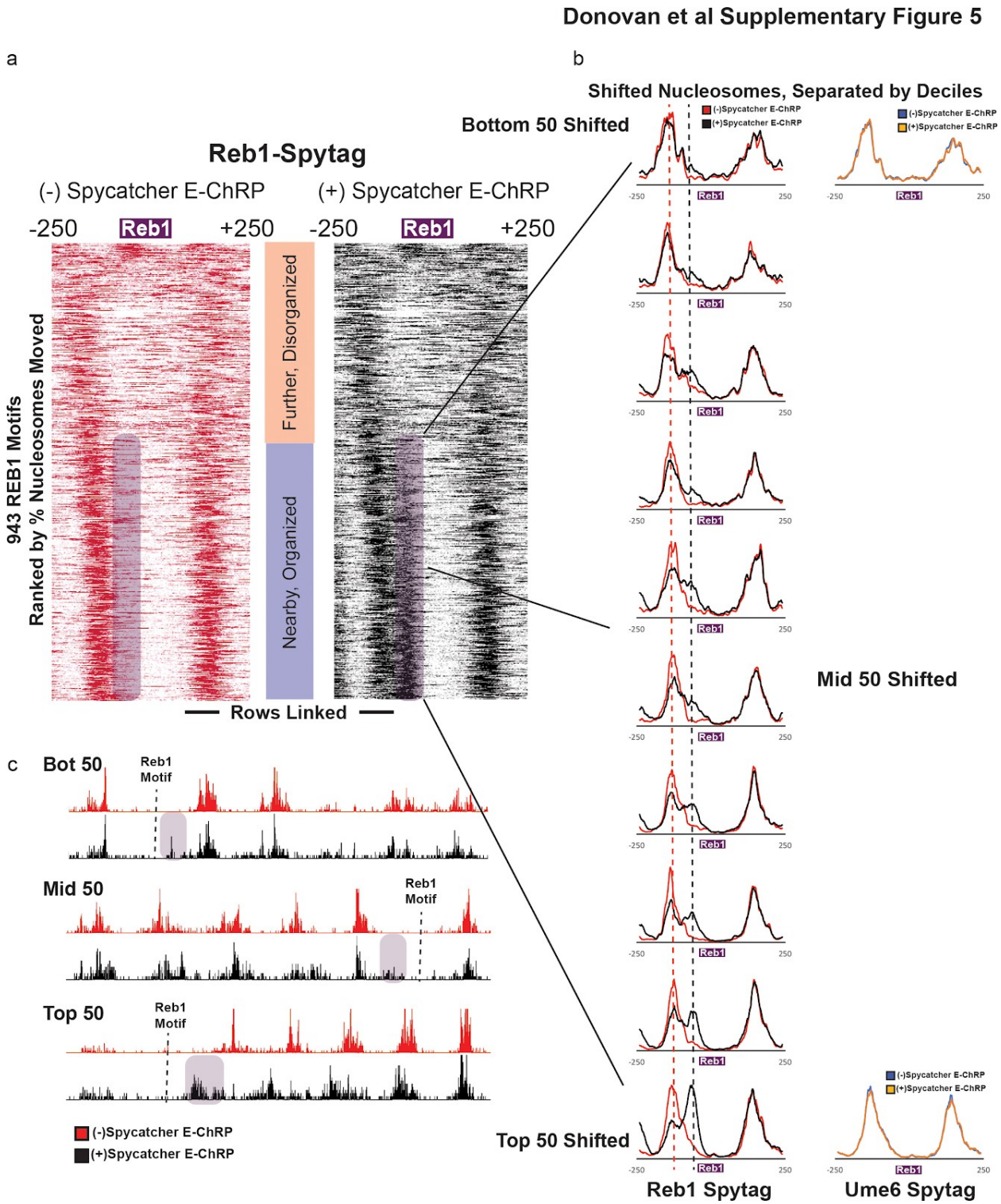

Supplementary Figure 5. Spycatcher E-ChRP Activity Varies at Reb1 Binding Sites.